THE JOURNAL OF BIOLOGICAL CHEMISTRY VOL. 291, NO. 36, pp. 18959–18966, September 2, 2016

Electrochemical Evidence for Neuroglobin Activity on NO at Physiological Concentrations*

Received for publication, March 30, 2016, and in revised form, July 7, 2016 Published, JBC Papers in Press, July 8, 2016, DOI 10.1074/jbc.M116.730176

Stanislav Trashin[‡], Mats de Jong[‡], Evi Luyckx[§], Sylvia Dewilde[§], and Karolien De Wael[‡1]

From the Departments of [‡]Chemistry and [§]Biomedical Sciences, University of Antwerp, 2010 Antwerp, Belgium

The true function of neuroglobin (Ngb) and, particularly, human Ngb (NGB) has been under debate since its discovery 15 years ago. It has been expected to play a role in oxygen binding/supply, but a variety of other functions have been put forward, including NO dioxygenase activity. However, *in vitro* studies that could unravel these potential roles have been hampered by the lack of an Ngb-specific reductase. In this work, we used electrochemical measurements to investigate the role of an intermittent internal disulfide bridge in determining NO oxidation kinetics at physiological NO concentrations. The use of a polarized electrode to efficiently interconvert the ferric (Fe^{3+}) and ferrous (Fe^{2+}) forms of an immobilized NGB showed that the disulfide bridge both defines the kinetics of NO dioxygenase activity and regulates appearance of the free ferrous deoxy-NGB, which is the redox active form of the protein in contrast to oxy-NGB. Our studies further identified a role for the distal histidine, interacting with the hexacoordinated iron atom of the heme, in oxidation kinetics. These findings may be relevant *in vivo*, for example, in blocking apoptosis by reduction of ferric cytochrome *c*, and gentle tuning of NO concentration in the tissues.

Neuroglobin (Ngb)[2] is the vertebrate globin that has been hypothesized to be involved in, *e.g.* O_2 binding/supply, the metabolism of reactive nitrogen and oxygen species, apoptosis through different pathways, intracellular signaling, and cell protection during hypoxia and ischemia (1–6). Besides the central and peripheral nervous system and retina, Ngb is also expressed in endocrine tissues, hematopoietic stem cells, the gastrointestinal tract, and cancer cells (7, 8). Although the first publication on the subject was in 2000, the *in vivo* role of Ngb is still uncertain. Studies on Ngb knock-out mice and regional gene expression did not clarify it further (3, 9–13), but most of the reports in the topic supported its neuroprotective function at least under conditions of neuroglobin overexpression (11, 14, 15). Some histological data additionally indicated that Ngb can be involved in regulation of the circadian rhythm (sleep-wake cycle) (12, 16) and protection of neurons from neurodegenerative disorders, such as Alzheimers disease (17–19). Obviously, further *in vivo* and *in vitro* studies of Ngb are necessary to clarify its molecular mechanisms of action.

As other globins, *e.g.* myoglobin and hemoglobin, Ngb displays the three-over-three α-helical sandwich structure. However, Ngb structurally differs somewhat from myoglobin and hemoglobin, suggesting a different functional destination for Ngb compared with the classic globins (20). Both its weak O_2 binding affinity under physiological conditions (21) and its hexacoordinated structure of the iron atom of the heme leading to a possible intrinsic binding competition with external gaseous ligands such as O_2, CO, and NO, support the hypothesis that Ngb is not constructed to transport or store O_2 (22). The unclear mechanism of action encourages researchers for detailed studies of Ngb structure and properties.

The well defined spectral properties of the heme in globins provide opportunities for studies by UV/visible and EPR (20, 23–25). Previously, myoglobin and hemoglobin have been extensively studied using electrochemical methods (26–30). However, electrochemistry has not yet been explored in studies of Ngb. Compared with other techniques, the electrochemical approach affords reduction or oxidation of Ngb by applying a potential to a working electrode without introduction of supplementary redox reagents.

Previously, two attempts were made to link NGB to electrode surfaces using modified gold and nanoporous indium tin oxide electrodes (31, 32). Although electric communication of NGB with the electrodes was confirmed through spectral changes in the immobilized protein, voltammetry measurements were impossible because of low protein surface coverage and slow electron transfer kinetics. Recently we designed an efficient protocol for immobilization and electrochemical measurements of small hydrophilic proteins including NGB (33). It created the opportunity for kinetic studies of NGB using voltammetry techniques.

Due to reactivity of the heme iron, NGB can act through multiple molecular mechanisms that seem to be closely related to the redox and ligation states of the iron (21, 34–50) (Fig. 1). Globins can express NO dioxygenase activity (oxidation of NO to nitrate in the presence of O_2 as shown in Fig. 1, reaction *d*). However, the relatively rapid autoxidation of Ngb (Fig. 1, reaction *c*) compels the introduction of a reductant or enzymatic reducing system to recover the ferrous form (Fig. 1, reaction *i*), which may interfere with measurements. Moreover, UV/visible assays need a 5–10 μM concentration of globins and an excess of NO, which exceeds by approximately 2 orders of magnitude the

* This work was supported by Fonds Wetenschappelijk Onderzoek (FWO) Grant G.0687.13 and Universiteit Antwerpen GOA BOF 28312. The authors declare that they have no conflicts of interest with the contents of this article.

[1] To whom correspondence should be addressed: Dept. of Chemistry, AXES Research Group, the University of Antwerp, Groenenborgerlaan 171, B-2010 Antwerp, Belgium. Tel.: 32-3-265-3335; E-mail: karolien.dewael@uantwerpen.be.

[2] The abbreviations used are: Ngb, neuroglobin; NGB, human neuroglobin; NGB*, NGB with mutated surface cysteines; NGB_{SS}, NGB with the internal disulfide bridge; CV, cyclic voltammetry; DPV, differential pulse voltammetry; BisTris, 2-[bis(2-hydroxyethyl)amino]-2-(hydroxymethyl)propane-1,3-diol.

NO concentration *in vivo* (51). The advantage of the electrochemical approach is that Ngb can be rapidly converted from the ferric (Fe^{3+}) to the ferrous (Fe^{2+}) form at a polarized electrode, which facilitates control of the redox state of the protein and monitoring following chemical reactions in the presence of possible substrates such as O_2 and NO. Moreover, when the protein is immobilized in a thin layer at the electrode surface, very low equilibrium concentrations of substrates can be introduced into the measuring cell without concern of its possible change because of reaction with the protein. The internal disulfide bridge between Cys-46 and Cys-55 in NGB defines oxygen-binding properties through the affinity of the distal His-64 (Fig. 1). The thiol/disulfide couple in NGB has a reduction potential of −0.194 V measured through equilibrium redox titration with glutathione (40). This value suggests that in a cell at normal conditions the disulfide bond is rather reduced (40), whereas the cysteine residues in the isolated protein are oxidized in air forming the disulfide bridge (21, 34).

The NGB with the disulfide bridge will be referred to as NGB_{SS}. To ease the study of NGB with the reduced disulfide bridge *in vitro*, a model protein with mutated surface cysteines (NGB*) was created (21, 52). NGB* behaves in a similar way to NGB with the reduced disulfide bond, but it allows to work without precautions against oxidation of the thiols into the disulfide bridge (21). In this work we compared the behavior of NGB_{SS} and NGB* to assess the effect of the disulfide bridge on the properties and mechanisms of action of NGB.

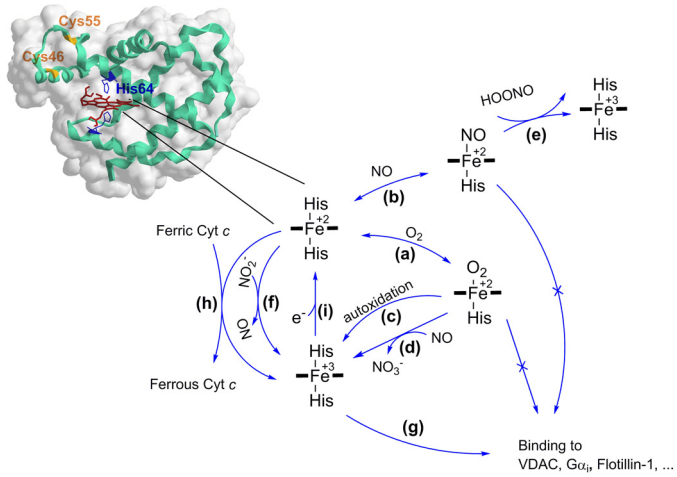

FIGURE 1. **The relationship of the redox and ligation states of the heme iron and NGB reactivity.** *a,* ferrous (Fe^{2+}) NGB reacts with O_2 to form the O_2 adduct. The dissociation of the distal histidine limits the binding kinetics due a low dissociation rate constant of 0.6 and 7 s^{-1} for NGB with reduced and oxidized states of the internal disulfide bridge, respectively (34, 35). The P_{50} value was reported in the range of 1–8 torr depending on pH, temperature, and the state of the internal disulfide bound (21). *b,* ferrous NGB reacts with NO leading to the nitrosyl ligated form with $K_d \approx 1$ nM and a slow dissociation rate constant $k_{off} \approx 10^{-4}$ to 10^{-3} s^{-1} (37). *c*, NGB-O_2 adduct is prone to autoxidation with $k \approx 0.17$ min^{-1} (21). Similar to myoglobin and hemoglobin, NGB has been reported as a scavenger of reactive oxygen and nitrogen species (*ROS*, *RNS*); *d*, NGB shows NO dioxygenase activity with $k_{cat} \approx 300$ s^{-1} (37, 38); *e*, nitrosyl ferrous NGB but not ferric (Fe^{3+}) NGB can scavenge peroxynitrite with $k_{cat} \approx 1.3 \times 10^5$ M^{-1} s^{-1} (39); *f*, ferrous (Fe^{2+}) NGB can reduce nitrite (NO_2^-) although with a relatively low rate constant of 0.06 and 0.12 M^{-1} s^{-1} for NGB with the reduced and oxidized states of the disulfide bridge, respectively (40). The role of NGB in blocking apoptosis through binding other proteins has been also suggested in the literature: *g*, NGB can bind to the GDP-bound form of the α-subunit of heterotrimeric G-protein (Gα$_i$) with $K_d \approx 6 \times 10^2$ nM (41). Immunoprecipitation techniques revealed binding of NGB to voltage-dependent anion channel (42), Flotillin-1 (43), two members of the Rho GTPase family (Rac1 and RhoA), as well as the Pak1 kinase (44), and a subunit of the mitochondrial complex III cytochrome c_1 (45). It has been found that the conformational transition in NGB upon binding ligands such as O_2 and NO can prevent NGB binding to Gα$_i$. Similar mechanisms may regulate binding to other proteins. *h*, moreover, ferrous NGB is capable to reduce rapidly ferric cytochrome *c* (Cyt *c*) with a kinetic constant of 2×10^7 M^{-1} s^{-1} (46), which seems to be facilitated by an appropriate docking between two proteins (47, 48). Interaction between Cyt *c* and NGB goes through a rapid transient binding with a relatively high dissociation constant, $K_d \approx 120$ μM (48), which decreases in low ionic strength buffer suggesting that the interaction is largely electrostatic in nature (48, 49). *i*, the reaction that is responsible for one-electron reduction of the ferric (Fe^{3+}) to ferrous (Fe^{2+}) form is not known yet. It can be driven by an enzyme process or a low molecular weight redox compound/mediator. Noteworthy, hexacoordination of the heme iron favors reduction kinetics comparing to pentacoordinated analogues (50).

Results

Electrochemical Behavior of NGB—Under N_2 atmosphere, NGB* showed highly reversible electrochemical behavior when either dissolved in solution or immobilized on the electrodes (Fig. 2). The redox process at a formal potential $E^{0'}$ of −0.136 ± 0.005 V corresponds to $Fe^{3+/2+}$ transition in the heme unit of NGB*. Because of hexacoordination of the iron, the heme unit undergoes little structural reorganization during the reduction/oxidation transition, enhancing electron transfer kinetics (50, 53). NGB_{SS} behaved similarly with a formal potential $E^{0'}$ of −0.126 ± 0.006 V, which we reported recently (33). A similar value was obtained by means of redox titration (−0.118 ± 0.004 V) (54). A slightly higher reduction potential of −0.103 V was assessed by spectroelectrochemical measurements of the protein adsorbed at a transparent nanoporous indium tin oxide electrode (32).

In equilibrium conditions, the protein will be reduced at potentials of the working electrode (*E*) lower than the formal potential ($E^{0'}$) and oxidized at higher ones according to the Nernst equation,

$$E = E^{0'} + 0.058 \times \lg([Ox]/[Red]) \qquad \text{(Eq. 1)}$$

where [Ox] and [Red] are the equilibrium concentrations of the oxidized and reduced forms.

It has been reported that NGB binds reversibly to O_2 (Fig. 1, reaction *a*) with a half-saturation pressure (P_{50}) of 1–8 mm Hg depending on pH, temperature, and the state of the internal disulfide bond (21). When the measuring buffer was saturated with air, the peak current of the heme unit in NGB* was suppressed (Fig. 2, *C* and *D*) due to formation of the oxy-form of NGB*. The loss of the redox activity is related to the formation of the charge-transfer state involving orbitals of Fe^{2+} and O_2 (55), which precludes the transition from Fe^{2+} to Fe^{3+} in the presence of O_2.

Effect of O_2 Concentration—The process of O_2 binding in NGB is preceded by a relatively slow distal histidine dissociation ($k = 7$ s^{-1} for NGB* and 0.6 s^{-1} for NGB_{SS} as measured by flash photolysis (34)) as represented in Scheme 1.

The slow O_2 association/dissociation kinetics allowed us to perform voltammetry measurements of the ferrous deoxy-NGB without a noticeable shift in the equilibrium between oxy and deoxy forms during the measurements. The constant position of the peak potential at different levels of O_2 suggests that

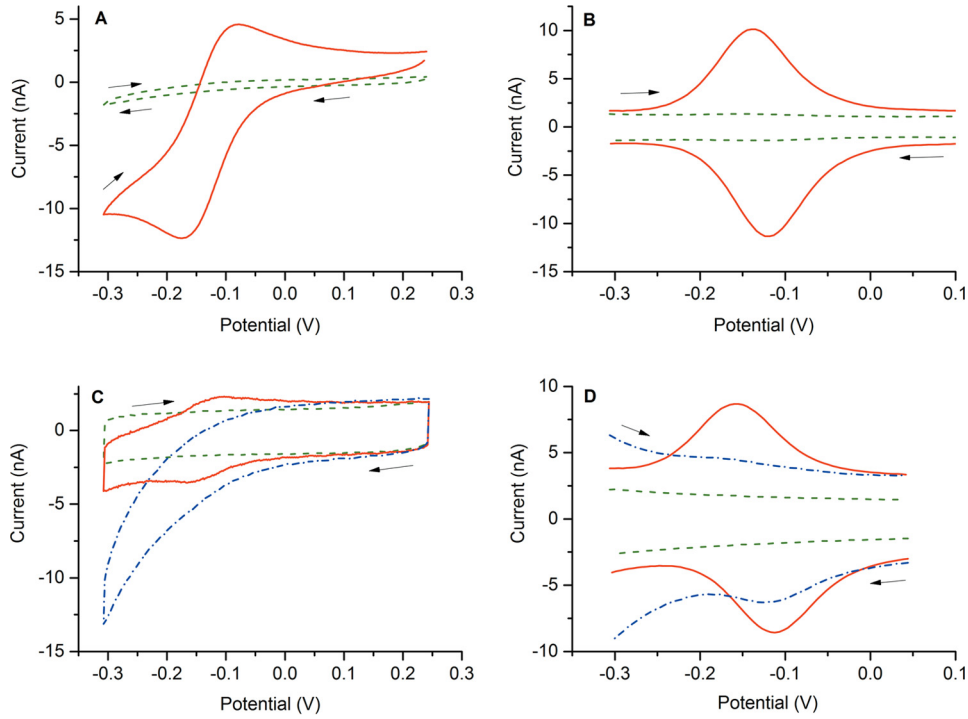

FIGURE 2. **CV and DPV behavior of NGB* in PBS buffer solution (*A* and *B*) and immobilized on the gold electrodes (*C* and *D*).** Concentration of the dissolved NGB*, 20 μM; surface density of the immobilized NGB*, 2 pmol/cm^2; CV scan rate, 20 mV/s; DPV modulation amplitude, 20 mV; modulation time, 0.05 s; interval time, 0.5 s. The *arrows* denote scan directions. Blank voltammograms are shown by *dashed lines* (in *green*) and *curves* recorded in the air-saturated buffer are presented by *dashed-dotted lines* (in *blue*).

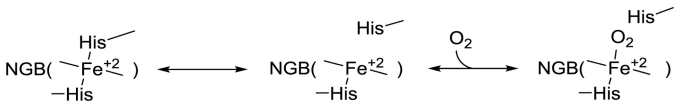

SCHEME 1

the kinetics of O_2 dissociation are relatively slow compared with the time scale of the performed electrochemical measurements (56). However, faster scan rates can be applied if necessary. Thus, the peak current must be proportional to the amount of deoxy-NGB and can be converted to the fraction of deoxy-NGB as $I_p/I_{p,0}$ or to the fraction of oxy-NGB as $(1 - I_p/I_{p,0})$, where $I_{p,0}$ is the peak current in the absence of O_2 and I_p is the peak current at a given level of O_2.

Fig. 3 shows the effect of oxygen concentration on the peak current for both NGB* and NGB_{SS}, obtained by DPV method. The plot of the oxy-NGB fraction against O_2 concentration is shown in Fig. 3*C*. The P_{50} was determined from the curves as 1.4 ± 0.5 torr for NGB_{SS} and 6.1 ± 1.3 torr for NGB*. Similar values were previously assessed in other studies (Table 1) based on flash photolysis and UV/visible measurements (21, 34).

Effect of Nitric Oxide—The effect of submicromolar NO concentration on NGB* and NGB_{SS} was studied in the presence of 30 torr (50 μM) of O_2, which is close to the normal level of O_2 in the brain (57). Fig. 4, *A* and *B*, represents the corresponding data. When 50 μM O_2 was introduced into the measuring cell, the peak current of NGB* was suppressed because of binding of NGB* with O_2, as described in the previous section.

Introduction of NO into the cell restored the peak current proportional to the NO concentration (Fig. 4, *A* and *B*). The increase in the peak current implies the increase of the steady-state concentration of the ferrous NGB*, which was accumulated because of slow distal histidine dissociation during the oxygen-binding reaction becoming the rate-limiting step of the ongoing reaction (Fig. 5*A*). In the concentration range of 0.50 – 0.75 μM NO, ~85% of NGB* was accumulated in the ferrous form (Fig. 4*C*). In these conditions the process was completely limited by O_2 binding and did not depend on NO concentration. At lower NO concentrations the amount of ferrous NGB was strictly proportional to the amount of NO.

It is noteworthy that NO concentrations higher than 1 μM resulted in a partial decrease in the ferrous NGB* fraction, which can be explained by inhibition of the heme by strongly bound NO (Fig. 1, reaction *b*). Fig. 4*D* shows the long-term effect of 1 μM NO in the presence of 30 μM O_2. Because of the high affinity and stability of the NGB*-NO complex (36), the level of ferrous NGB* decreased by 60%. The initial level could not be restored by increasing the O_2 concentration or N_2 purging, probably because of the slow NO dissociation ($k_{off} = 2 \times 10^{-4}$ s^{-1}) from the complex (36).

Surprisingly, NGB_{SS} demonstrated only a minor increase of the ferrous NGB_{SS} fraction with the NO concentration in the same conditions as NGB* (Fig. 4*C*). The fraction of ferrous deoxy-NGB_{SS} was 13 and 18% for 0.5 and 1.0 μM NO, respectively. As Fig. 5*B* illustrates, the disulfide bridge increased the rate of His(E7) dissociation and, apparently, shifted the rate-limiting step from O_2 binding to the NO oxidation.

Discussion

A reductase that is capable of rapidly reducing NGB is not yet known. This problem limits assay studies because of autoxida-

tion of NGB in the presence of O_2. In this work we employed a polarized electrode as the reducing system that can recover the ferrous NGB from the oxidized ferric form. Such an approach allowed rapid reduction of the protein without introduction of any chemicals and simplified the study.

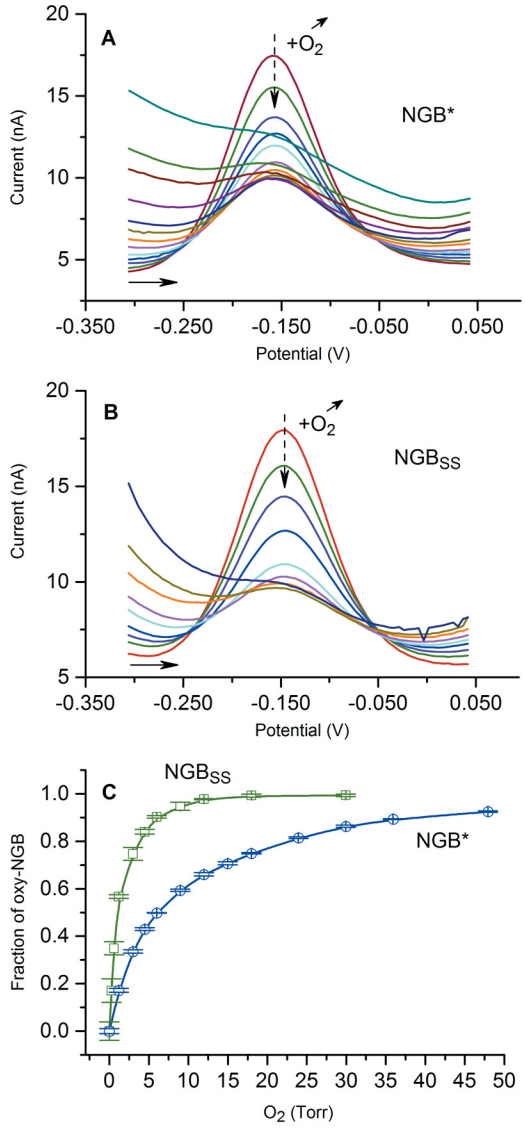

FIGURE 3. **Behavior of NGB in the presence of different levels of O_2.** *A* and *B*, change in voltammograms with an increase of O_2 level in the presence of NGB* and NGB_{SS}; *C*, determined fraction of the oxygenated NGB in equilibrium with the ferrous (Fe^{+2}) NGB as a function of O_2 concentration. *Error bars* show standard deviation for three consecutive measurements. PBS, pH 7.4, 25 °C.

The technique for studying redox proteins on an electrode, also known as protein film voltammetry (58, 59), was previously widely used for mechanistic studies of redox proteins. However, small hydrophilic proteins can easily desorb and dissolve in bulk. Thus, an appropriate immobilization technique must be used. Recently, we developed a gentle immobilization procedure based on a bis-silane cross-linker dissolved in water medium (33). Immobilized proteins including NGB could be retained at the surface without loss of redox activity or a noticeable shift of their redox potentials. Fast electron transfer kinetics allows us to reduce the protein rapidly and without diffusion limitation. Moreover, because of the small amount of the protein (~0.04 pmol/electrode) and the large bulk volume, the consumption of O_2 and NO from the bulk is negligible even when their concentrations are low. It permits reliable measurements for low concentrations of NO and O_2, whereas in assays using about 10 μM protein concentration, studies in the presence of submicrololar NO would be impossible. Thus, the suggested approach allows 1) rapid electrochemical reduction of NGB and 2) equilibrium and kinetic measurements in low NO and O_2 concentration ranges.

It is known that the disulfide bridge regulates the affinity of NGB to bind oxygen (34). To study this effect a comparison was made between the wild type NGB (NGB_{SS}) and NGB with mutated cysteines (NGB*) (21, 34). As ferrous NGB alone is electroactive but its complex with O_2 is not, we could titrate the protein by adding O_2 similar to the method used in UV/visible assays but without introduction of any reduction agents. The obtained values of P_{50} were 6.1 ± 1.3 and 1.4 ± 0.5 torr for NGB* and NGB_{SS}, respectively, which is in good agreement with other reports (Table 1).

It should be mentioned that the published P_{50} values demonstrate a noticeable distribution. Moreover, one may notice a difference in reports regarding the temperature dependence of O_2 affinity in NGB measured by equilibrium titration and flash photolysis (21, 60). The results obtained in UV/visible assays could depend on the rate of autoxidation of NGB and efficiency of the reducing system used at particular pH values and temperatures. The suggested electrochemical approach is free from these complications and can be further used for more detailed studies of the affinity of NGB to bind O_2 or other gases in different conditions.

Affinity to O_2 that is regulated through the disulfide bond is an intriguing feature of NGB but its role in O_2 supply/storage is unlikely for many reasons (3, 4). The role of NGB as a possible NO dioxygenase is more supported because such a function is

TABLE 1
Comparison of P_{50} values for NGB obtained by different methods

	Method	Conditions	P50 (Torr)	Reference
NGB*	Voltammetry	PBS, pH 7.4, 25 °C	6.1 ± 1.3[a]	This work
NGB_{SS}	Voltammetry	PBS, pH 7.4, 25 °C	1.4 ± 0.5[a]	This work
NGB*[b]	Equilibrium UV/visible[c]	BisTris//Hepes, pH 7.0, 25 °C	5	Fago *et al.* (21)
NGB*[b]	Equilibrium UV/visible[c]	BisTris//Hepes, pH 7.6, 20 °C	2.6	Fago *et al.* (21)
NGB_{SS}	Equilibrium UV/visible[c]	BisTris//Hepes, pH 7.6, 20 °C	0.67	Fago *et al.* (21)
NGB*	Flash photolysis	Phosphate, pH 7.0, 25 °C	10	Hamdane *et al.* (34)
NGB_{SS}	Flash photolysis	Phosphate, pH 7.0, 25 °C	0.9	Hamdane *et al.* (34)
NGB + DTT	Flash photolysis	Phosphate, pH 7.0, 25 °C	8.4	Hamdane *et al.* (34)

[a] Average ± S.E. (n = 4).
[b] No difference between NGB* and NGB + DTT was reported.
[c] Measured on an ultrathin layer of protein sample using a gas diffusion chamber.

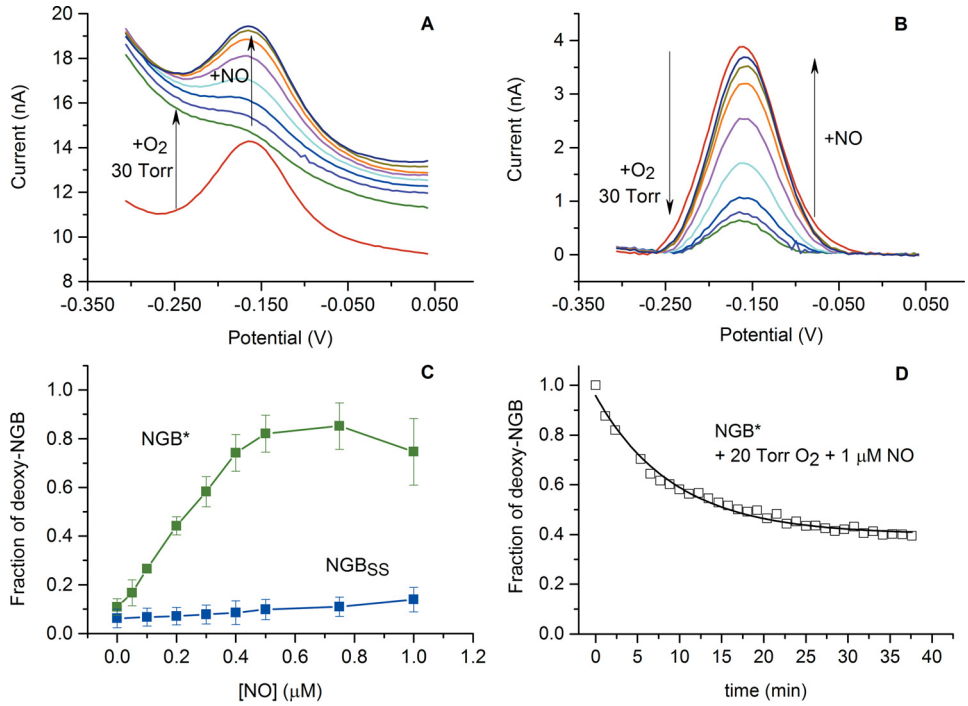

FIGURE 4. **Behavior of NGB in the presence of 30 torr O_2 and submicromolar NO concentrations.** *A,* change in DPV curves for NGB*; *B,* the DPV curves after baseline correction; *C,* dependence of the steady state deoxy-NGB fraction on NO concentration in the presence of 30 torr O_2. Average values of three separate titration curves are plotted, with standard deviation values. *D,* stability of deoxy-NGB* in the presence of 20 torr O_2 and 1 μM NO. *Arrows* denote direction of changes. PBS, pH 7.4, 25 °C.

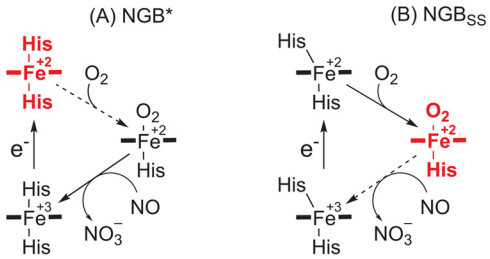

FIGURE 5. **The mechanism of NGB transitions in the presence of 0.5 μM NO and 30 torr O_2.** *A,* behavior of NGB*, which models the protein with the opened disulfide bridge that favors the hexacoordinate ferrous form; *B,* behavior of NGB_{SS}, which is the protein with the disulfide bridge that favors the oxygenated form. *Broken arrows* indicate a rate-limiting step and the *bold red* structures depict an accumulated form.

well known for hemoglobin, myoglobin, and especially for flavohemoglobin (61).

To the best of the authors' knowledge, only two works have been published with regard to an *in vitro* test of dioxygenase function in Ngb in the presence of O_2, conducted with mouse Ngb in air-saturated buffer (37) and with human NGB in the presence of 4% (30 torr) O_2 (38). In both works the authors reported rapid NO oxidation by oxy-Ngb ($k \approx 300\ s^{-1}$), which followed the rate-limiting distal histidine dissociation and O_2 binding ($k \approx 0.4\ s^{-1}$) (37). The measurements with mouse Ngb were performed with 10 and 250 μM NO, and the total kinetics were independent of NO concentration (37). The measurements with NGB by Smagghe *et al.* (38) were conducted in the presence of 40 μM NO. The ability to catalytically scavenge NO was directly related to the recovery rate of the ferrous form by the reduction system used. No data regarding physiologically relevant NO concentrations or an effect of the disulfide bond have yet been reported. In contrast to the previous works (37, 38), we were able to do measurements in a low NO concentration range and overcome the limitation of the slow re-reduction of NGB from its ferric form.

As a result, we found that O_2 binding kinetics in NGB* are comparable with an NO oxidation rate up to 0.5 μM NO concentration, which resulted in a split of the NGB* into deoxy- and oxy-NGB* fractions proportional to NO concentration. When the NO concentration was 0.5 μM or higher, the kinetics of the dioxygenase activity were fully limited by O_2 binding, and almost all NGB* was accumulated in the free ferrous form. In the same conditions, NGB_{SS} did not show a similar effect, most probably because of the faster formation of the oxy form because of the 10-fold faster distal histidine dissociation (34).

In conclusion, we demonstrated a new approach to study NGB in the presence of O_2 and NO that overcomes the limitation related to autoxidation of the protein and allows to work with submicromolar concentrations of effectors. The approach can be potentially extended to other hexacoordinate globins. If we postulate the existence of a rapid reducing system for NGB *in vivo* (which should exist because of noticeable autoxidation of the protein in the presence of O_2), then not only affinity to bind O_2 but also the rate of NO oxidation to NO_3^- and accumulation of the ferrous NGB is defined by the state of the internal disulfide bridge and NO concentration.

When the bridge is reduced, NGB can exist in the ferrous form even at high O_2 concentrations when a near micromolar or submicromolar amount of NO is present. This could be meaningful *in vivo*. For example, reduction of ferric cytochrome *c*, which has been hypothesized as an anti-apoptotic mechanism of action for NGB (46, 47), can be accomplished only by the ferrous deoxy-NGB. Moreover, the ligand binding

induces structural transition in NGB that prevents formation of the stable complex with $G\alpha_i$ (41) and, probably, other apoptosis-related proteins (Fig. 1, reaction *g*). In the conditions of severe hypoxia, the NGB-O_2 adduct can dissociate to form ferrous NGB. However, it may probably lose the ability to interact with the apoptosis-related proteins due to binding of NO whose concentration is elevated under hypoxia conditions. Our data suggest that ferrous (Fe^{2+}) NGB can appear at a certain ratio of NO/O_2 concentrations and thus, reduce the ferric cytochrome *c* or bind the proteins involved in apoptosis (41–45), thus, leading to protection against neuronal death.

Finally, it is worth noting that NO plays multiple roles in the nervous system and in the pathophysiology of several neurological disorders (62). It can be assumed that NGB gently regulates the NO concentration or acts as a sensor of NO/O_2 ratio in cells, generating a redox active form of NGB from the redox inactive oxy-form, which exists at normal O_2 and very low NO concentrations.

Experimental Procedures

Materials—Recombinant human Ngb (NGB) and the triple mutant with replaced cysteine residues (C46G, C55S, and C120S; NGB*) were expressed and purified as described previously (52). Briefly, the recombinant expression plasmid with the pET3a vector was transformed in the *Escherichia coli* strain BL21(DE3)pLysS. The cells were grown overnight at 37 °C in 6 ml of L-broth containing ampicillin and chloramphenicol. Then, the culture was transferred into 250 ml of TB medium containing ampicillin, chloramphenicol, and δ-aminolevulinic acid. After reaching $A_{600} = 0.8$, the expression was induced by isopropyl 1-thio-D-galactopyranoside and continued overnight. After the preparation of a crude protein extract, NGB was purified using DEAE-Sepharose Fast Flow and Sephacryl S-200 High Resolution chromatography, dialyzed against 5 mM Tris-HCl, pH 8.5, and concentrated.

Inorganic salts, NaOH, H_2SO_4, and 1,2-bis(trimethoxysilyl)ethane were purchased from Sigma (Belgium). 6-Mercapto-1-hexanol (>98.0%) was sourced from TCI Europe N.V. (Belgium).

Preparation of Electrodes—The commercial gold disk electrodes, 1.6-mm diameter (BASi, West Lafayette, IN), were polished first on nylon pads (Buehler, Lake Bluff, IL) using diamond suspensions of 3-, 1-, and 0.25-μm particle size (DP-Spray, Struers, Ballerup, Denmark) in a supplier recommended lubricant (DP-Lubricant, Struers, Ballerup, Denmark), and on soft pads (Buehler) using a water-based γ-alumina slurry of 50-nm particle size (SPI Supplies, West Chester, PA). The electrodes were sonicated in ethanol and ultrapure water after each polishing step. Next, the electrodes were electrochemically treated in 0.5 M NaOH and 0.5 M H_2SO_4 until a repetitive voltammogram of polycrystalline gold was achieved (63, 64). Finally, the electrodes were left in 8 mM 6-mercapto-1-hexanol solution in ultrapure water for ~20 h.

Afterward, 1.8 μl of a mixture consisting of 15 μM protein and 10 mM 1,2-bis(trimethoxysilyl)ethane in 50 mM KH_2PO_4 buffer, pH 7, was placed on the electrodes and dried at room temperature for 1 h. The obtained surface coverage of the surface-confined NGB was ~2 pmol/cm^2.

Cyclic (CV) and differential pulse voltammetry (DPV) were conducted in PBS buffer, pH 7.4, using a conventional three-electrode cell and μAutolab III electrochemical interface (Metrohm-Autolab BV, the Netherlands). A saturated calomel electrode (Radiometer, Denmark; +0.244 V *versus* standard hydrogen electrode at 25 °C) and a glassy carbon rod were used as reference and counterelectrode, respectively. All potentials are given *versus* the standard hydrogen electrode.

Background CV behavior of MH-modified electrodes was carefully checked to ensure the quality of the electrode preparation and stability of the electrodes. Contaminated electrodes and electrodes with a defective MH layer (which could be disclosed due to an increased background current under N_2 atmosphere) demonstrated inappropriate long-term stability and were discarded.

O_2 Binding—The measuring buffer (30 ml) was purged with N_2 for 1 h in advance and for at least 20 min after the protein electrodes were inserted into the thermostatic (25.0 ± 0.2 °C) electrochemical cell. CV and DPV performances of the electrodes were recorded to ensure good stability and appropriate immobilization of NGB. Next, DPV curves were sequentially recorded starting from −0.3 until +0.05 V with a conditioning step of 1 min before each measurement, when the potential was set again to −0.3 V to keep the protein in the reduced form. After recording at least five consecutive DPV curves under N_2 to ensure stable peak intensity, a certain volume of the air-saturated buffer, equilibrated at the same temperature, was injected using an air-tight syringe. For each concentration the measurements were repeated at least twice to ensure the stable value of the peak current after introduction of O_2.

NO Metabolism—A saturated water solution of NO was prepared as previously described (65, 66). Briefly, 2 M H_2SO_4 was carefully added dropwise into saturated $NaNO_2$ preliminarily purged with nitrogen. The disproportional reaction resulted in the formation of NO, which was directed to pass through a washing bottle containing 30% NaOH and two vials with ultrapure water. The solution from the second vial was used in the experiments. Under room temperature (22 °C) and normal pressure conditions, the saturated concentration of NO in water is close to 2.0 mM (67). Saturated NO solution was added to the electrochemical cell using an air-tight Hamilton syringe to get NO concentrations in the range from 0.05 to 1.25 μM. The measurements were done in the presence of 50 μM (30 torr) O_2 at 25 °C.

Author Contributions—K. D. W. and S. T. designed research and analyzed all data; S. T. conducted most of the experiments and wrote most of the paper; M. d. J. conducted preliminary experiments on the immobilization and electrochemical characterization of NGB; E. L. purified and characterized samples of NGB and NGB*, S. D. contributed to the interpretation of data and revised the paper.

References

1. Burmester, T., Weich, B., Reinhardt, S., and Hankeln, T. (2000) A vertebrate globin expressed in the brain. *Nature* **407,** 520–523
2. Tejero, J., and Gladwin, M. T. (2014) The globin superfamily: functions in nitric oxide formation and decay. *Biol. Chem.* **395,** 631–639

3. Burmester, T., and Hankeln, T. (2014) Function and evolution of vertebrate globins. *Acta Physiol.* **211,** 501–514
4. Ascenzi, P., Gustincich, S., and Marino, M. (2014) Mammalian nerve globins in search of functions. *IUBMB Life* **66,** 268–276
5. Haines, B., Demaria, M., Mao, X., Xie, L., Campisi, J., Jin, K., and Greenberg, D. A. (2012) Hypoxia-inducible factor-1 and neuroglobin expression. *Neurosci. Lett.* **514,** 137–140
6. Jin, K., Mao, X. O., Xie, L., Khan, A. A., and Greenberg, D. A. (2008) Neuroglobin protects against nitric oxide toxicity. *Neurosci. Lett.* **430,** 135–137
7. Emara, M., Turner, A. R., and Allalunis-Turner, J. (2010) Hypoxic regulation of cytoglobin and neuroglobin expression in human normal and tumor tissues. *Cancer Cell Int.* **10,** 33
8. Fiocchetti, M., Nuzzo, M. T., Totta, P., Acconcia, F., Ascenzi, P., and Marino, M. (2014) Neuroglobin, a pro-survival player in estrogen receptor α-positive cancer cells. *Cell Death Dis.* **5,** e1449
9. Fordel, E., Thijs, L., Moens, L., and Dewilde, S. (2007) Neuroglobin and cytoglobin expression in mice: evidence for a correlation with reactive oxygen species scavenging. *FEBS J.* **274,** 1312–1317
10. Hundahl, C. A., Luuk, H., Ilmjärv, S., Falktoft, B., Raida, Z., Vikesaa, J., Friis-Hansen, L., and Hay-Schmidt, A. (2011) Neuroglobin-deficiency exacerbates Hif1A and c-FOS response, but does not affect neuronal survival during severe hypoxia *in vivo*. *PLoS ONE* **6,** e28160
11. Raida, Z., Hundahl, C. A., Kelsen, J., Nyengaard, J. R., and Hay-Schmidt, A. (2012) Reduced infarct size in neuroglobin-null mice after experimental stroke *in vivo*. *Exp. Transl. Stroke Med.* **4,** 15
12. Hundahl, C. A., Allen, G. C., Hannibal, J., Kjaer, K., Rehfeld, J. F., Dewilde, S., Nyengaard, J. R., Kelsen, J., and Hay-Schmidt, A. (2010) Anatomical characterization of cytoglobin and neuroglobin mRNA and protein expression in the mouse brain. *Brain Res.* **1331,** 58–73
13. Schmidt-Kastner, R., Haberkamp, M., Schmitz, C., Hankeln, T., and Burmester, T. (2006) Neuroglobin mRNA expression after transient global brain ischemia and prolonged hypoxia in cell culture. *Brain Res.* **1103,** 173–180
14. Fiocchetti, M., De Marinis, E., Ascenzi, P., and Marino, M. (2013) Neuroglobin and neuronal cell survival. *Biochim. Biophys. Acta* **1834,** 1744–1749
15. Raida, Z., Hundahl, C. A., Nyengaard, J. R., and Hay-Schmidt, A. (2013) Neuroglobin over expressing mice: expression pattern and effect on brain ischemic infarct size. *PLoS ONE* **8,** e76565
16. Hundahl, C. A., Fahrenkrug, J., Hay-Schmidt, A., Georg, B., Faltoft, B., and Hannibal, J. (2012) Circadian behaviour in neuroglobin deficient mice. *PLoS ONE* **7,** e34462
17. Khan, A. A., Mao, X. O., Banwait, S., Jin, K., and Greenberg, D. A. (2007) Neuroglobin attenuates β-amyloid neurotoxicity *in vitro* and transgenic Alzheimer phenotype *in vivo*. *Proc. Natl. Acad. Sci. U.S.A.* **104,** 19114–19119
18. Chen, L.-M., Xiong, Y.-S., Kong, F.-L., Qu, M., Wang, Q., Chen, X.-Q., Wang, J.-Z., and Zhu, L.-Q. (2012) Neuroglobin attenuates Alzheimer-like tau hyperphosphorylation by activating Akt signaling. *J. Neurochem.* **120,** 157–164
19. Ferrer, I., Gómez, A., Carmona, M., Huesa, G., Porta, S., Riera-Codina, M., Biagioli, M., Gustincich, S., and Aso, E. (2011) Neuronal hemoglobin is reduced in Alzheimer's disease, argyrophilic grain disease, Parkinson's disease, and dementia with Lewy bodies. *J. Alzheimers Dis.* **23,** 537–550
20. Dewilde, S., Kiger, L., Burmester, T., Hankeln, T., Baudin-Creuza, V., Aerts, T., Marden, M. C., Caubergs, R., and Moens, L. (2001) Biochemical characterization and ligand binding properties of neuroglobin, a novel member of the globin family. *J. Biol. Chem.* **276,** 38949–38955
21. Fago, A., Hundahl, C., Dewilde, S., Gilany, K., Moens, L., and Weber, R. E. (2004) Allosteric regulation and temperature dependence of oxygen binding in human neuroglobin and cytoglobin: molecular mechanisms and physiological significance. *J. Biol. Chem.* **279,** 44417–44426
22. Hankeln, T., Ebner, B., Fuchs, C., Gerlach, F., Haberkamp, M., Laufs, T. L., Roesner, A., Schmidt, M., Weich, B., Wystub, S., Saaler-Reinhardt, S., Reuss, S., Bolognesi, M., De Sanctis, D., Marden, M. C., *et al.* (2005) Neuroglobin and cytoglobin in search of their role in the vertebrate globin family. *J. Inorg. Biochem.* **99,** 110–119
23. Van Doorslaer, S., Trandafir, F., Harmer, J. R., Moens, L., and Dewilde, S. (2014) EPR analysis of cyanide complexes of wild-type human neuroglobin and mutants in comparison to horse heart myoglobin. *Biophys. Chem.* **190,** 8–16
24. Walker, F. A. (2006) The heme environment of mouse neuroglobin: histidine imidazole plane orientations obtained from solution NMR and EPR spectroscopy as compared with x-ray crystallography. *J. Biol. Inorg. Chem.* **11,** 391–397
25. Vinck, E., Van Doorslaer, S., Dewilde, S., Mitrikas, G., Schweiger, A., and Moens, L. (2006) Analyzing heme proteins using EPR techniques: the heme-pocket structure of ferric mouse neuroglobin. *J. Biol. Inorg. Chem.* **11,** 467–475
26. Fan, C., Chen, X., Li, G., Zhu, J., Zhu, D., and Scheer, H. (2000) Direct electrochemical characterization of the interaction between haemoglobin and nitric oxide. *Phys. Chem. Chem. Phys.* **2,** 4409–4413
27. Scheller, F. W., Bistolas, N., Liu, S., Jänchen, M., Katterle, M., and Wollenberger, U. (2005) Thirty years of haemoglobin electrochemistry. *Adv. Colloid Interface Sci.* **116,** 111–120
28. Kroning, S., Scheller, F. W., Wollenberger, U., and Lisdat, F. (2004) Myoglobin-clay electrode for nitric oxide (NO) detection in solution. *Electroanalysis* **16,** 253–259
29. Taniguchi, I., Watanabe, K., Tominaga, M., and Hawkridge, F. M. (1992) Direct electron transfer of horse heart myoglobin at an indium oxide electrode. *J. Electroanal. Chem.* **333,** 331–338
30. King, B. C., Hawkridge, F. M., and Hoffman, B. M. (1992) Electrochemical studies of cyanometmyoglobin and metmyoglobin: implications for long-range electron-transfer in proteins. *J. Am. Chem. Soc.* **114,** 10603–10608
31. Balland, V., Lecomte, S., and Limoges, B. (2009) Characterization of the electron transfer of a ferrocene redox probe and a histidine-tagged hemoprotein specifically bound to a nitrilotriacetic-terminated self-assembled monolayer. *Langmuir* **25,** 6532–6542
32. Schaming, D., Renault, C., Tucker, R. T., Lau-Truong, S., Aubard, J., Brett, M. J., Balland, V., and Limoges, B. (2012) Spectroelectrochemical characterization of small hemoproteins adsorbed within nanostructured mesoporous ITO electrodes. *Langmuir* **28,** 14065–14072
33. Trashin, S., de Jong, M., Meynen, V., Dewilde, S., and De Wael, K. (2016) Attaching redox proteins onto electrode surfaces by bis-silane. *ChemElectroChem* **7,** 1035–1038
34. Hamdane, D., Kiger, L., Dewilde, S., Green, B. N., Pesce, A., Uzan, J., Burmester, T., Hankeln, T., Bolognesi, M., Moens, L., and Marden, M. C. (2003) The redox state of the cell regulates the ligand binding affinity of human neuroglobin and cytoglobin. *J. Biol. Chem.* **278,** 51713–51721
35. Kiger, L., Uzan, J., Dewilde, S., Burmester, T., Hankeln, T., Moens, L., Hamdane, D., Baudin-Creuza, V., and Marden, M. (2004) Neuroglobin ligand binding kinetics. *IUBMB Life* **56,** 709–719
36. Van Doorslaer, S., Dewilde, S., Kiger, L., Nistor, S. V., Goovaerts, E., Marden, M. C., and Moens, L. (2003) Nitric oxide binding properties of neuroglobin: a characterization by EPR and flash photolysis. *J. Biol. Chem.* **278,** 4919–4925
37. Brunori, M., Giuffrè, A., Nienhaus, K., Nienhaus, G. U., Scandurra, F. M., and Vallone, B. (2005) Neuroglobin, nitric oxide, and oxygen: functional pathways and conformational changes. *Proc. Natl. Acad. Sci. U.S.A.* **102,** 8483–8488
38. Smagghe, B. J., Trent, J. T., 3rd, and Hargrove, M. S. (2008) NO dioxygenase activity in hemoglobins is ubiquitous *in vitro*, but limited by reduction *in vivo*. *PLoS ONE* **3,** e2039
39. Herold, S., Fago, A., Weber, R. E., Dewilde, S., and Moens, L. (2004) Reactivity studies of the Fe(III) and Fe(II)NO forms of human neuroglobin reveal a potential role against oxidative stress. *J. Biol. Chem.* **279,** 22841–22847
40. Tiso, M., Tejero, J., Basu, S., Azarov, I., Wang, X., Simplaceanu, V., Frizzell, S., Jayaraman, T., Geary, L., Shapiro, C., Ho, C., Shiva, S., Kim-Shapiro, D. B., and Gladwin, M. T. (2011) Human neuroglobin functions as a redox-regulated nitrite reductase. *J. Biol. Chem.* **286,** 18277–18289
41. Wakasugi, K., Nakano, T., and Morishima, I. (2003) Oxidized human neuroglobin acts as a heterotrimeric Gα protein guanine nucleotide dissociation inhibitor. *J. Biol. Chem.* **278,** 36505–36512
42. Yu, Z., Liu, N., Li, Y., Xu, J., and Wang, X. (2013) Neuroglobin overexpres-

sion inhibits oxygen-glucose deprivation-induced mitochondrial permeability transition pore opening in primary cultured mouse cortical neurons. *Neurobiol. Dis.* **56,** 95–103
43. Wakasugi, K., Nakano, T., Kitatsuji, C., and Morishima, I. (2004) Human neuroglobin interacts with flotillin-1, a lipid raft microdomain-associated protein. *Biochem. Biophys. Res. Commun.* **318,** 453–460
44. Khan, A. A., Mao, X. O., Banwait, S., DerMardirossian, C. M., Bokoch, G. M., Jin, K., and Greenberg, D. A. (2008) Regulation of hypoxic neuronal death signaling by neuroglobin. *FASEB J.* **22,** 1737–1747
45. Yu, Z., Zhang, Y., Liu, N., Yuan, J., Lin, L., Zhuge, Q., Xiao, J., and Wang, X. (2016) Roles of neuroglobin binding to mitochondrial complex III subunit cytochrome *c*1 in oxygen-glucose deprivation-induced neurotoxicity in primary neurons. *Mol. Neurobiol.* **53,** 3249–3257
46. Fago, A., Mathews, A. J., Moens, L., Dewilde, S., and Brittain, T. (2006) The reaction of neuroglobin with potential redox protein partners cytochrome b_5 and cytochrome *c*. *FEBS Lett.* **580,** 4884–4888
47. Raychaudhuri, S., Skommer, J., Henty, K., Birch, N., and Brittain, T. (2010) Neuroglobin protects nerve cells from apoptosis by inhibiting the intrinsic pathway of cell death. *Apoptosis* **15,** 401–411
48. Bønding, S. H., Henty, K., Dingley, A. J., and Brittain, T. (2008) The binding of cytochrome c to neuroglobin: a docking and surface plasmon resonance study. *Int. J. Biol. Macromol.* **43,** 295–299
49. Tiwari, P. B., Astudillo, L., Pham, K., Wang, X. W., He, J., Bemad, S., Derrien, V., Sebban, P., Miksovska, J., and Darici, Y. (2015) Characterization of molecular mechanism of neuroglobin binding to cytochrome *c*: a surface plasmon resonance and isothermal titration calorimetry study. *Inorg. Chem. Commun.* **62,** 37–41
50. Weiland, T. R., Kundu, S., Trent, J. T., 3rd, Hoy, J. A., and Hargrove, M. S. (2004) Bis-histidyl hexacoordination in hemoglobins facilitates heme reduction kinetics. *J. Am. Chem. Soc.* **126,** 11930–11935
51. Hall, C. N., and Garthwaite, J. (2009) What is the real physiological NO concentration *in vivo*? *Nitric Oxide* **21,** 92–103
52. Dewilde, S., Mees, K., Kiger, L., Lechauve, C., Marden, M. C., Pesce, A., Bolognesi, M., and Moens, L. (2008) Expression, purification, and crystallization of neuro- and cytoglobin. *Methods Enzymol.* **436,** 341–357
53. Kiger, L., Tilleman, L., Geuens, E., Hoogewijs, D., Lechauve, C., Moens, L., Dewilde, S., and Marden, M. C. (2011) Electron transfer function *versus* oxygen delivery: a comparative study for several hexacoordinated globins across the animal kingdom. *PLoS ONE* **6,** e20478
54. Tejero, J., Sparacino-Watkins, C. E., Ragireddy, V., Frizzell, S., and Gladwin, M. T. (2015) Exploring the mechanisms of the reductase activity of neuroglobin by site-directed mutagenesis of the heme distal pocket. *Biochemistry* **54,** 722–733
55. Chen, H., Ikeda-Saito, M., and Shaik, S. (2008) Nature of the Fe-O_2 bonding in oxy-myoglobin: effect of the protein. *J. Am. Chem. Soc.* **130,** 14778–14790
56. Gulaboski, R., Mirčeski, V., Lovrić, M., and Bogeski, I. (2005) Theoretical study of a surface electrode reaction preceded by a homogeneous chemical reaction under conditions of square-wave voltammetry. *Electrochem. Commun.* **7,** 515–522
57. Carreau, A., El Hafny-Rahbi, B., Matejuk, A., Grillon, C., and Kieda, C. (2011) Why is the partial oxygen pressure of human tissues a crucial parameter? small molecules and hypoxia. *J. Cell. Mol. Med.* **15,** 1239–1253
58. Armstrong, F. A., Heering, H. A., and Hirst, J. (1997) Reaction of complex metalloproteins studied by protein-film voltammetry. *Chem. Soc. Rev.* **26,** 169–179
59. Gulaboski, R., Mirčeski, V., Bogeski, I., and Hoth, M. (2011) Protein film voltammetry: electrochemical enzymatic spectroscopy: a review on recent progress. *J. Solid State Electrochem.* **16,** 2315–2328
60. Uzan, J., Dewilde, S., Burmester, T., Hankeln, T., Moens, L., Hamdane, D., Marden, M. C., and Kiger, L. (2004) Neuroglobin and other hexacoordinated hemoglobins show a weak temperature dependence of oxygen binding. *Biophys. J.* **87,** 1196–1204
61. Gardner, P. R. (2005) Nitric oxide dioxygenase function and mechanism of flavohemoglobin, hemoglobin, myoglobin and their associated reductases. *J. Inorg. Biochem.* **99,** 247–266
62. Jain, K. K. (2013) Role of nitric oxide in neurological disorders. in *Applications of Biotechnology in Neurology* (Jain, K. K., ed) pp. 249–282, Humana Press, New York
63. Juodkazis, K., Juodkazyt, J., Šebeka, B., and Lukinskas, A. (1999) Cyclic voltammetric studies on the reduction of a gold oxide surface layer. *Electrochem. Commun.* **1,** 315–318
64. Piela, B., and Wrona, P. K. (1995) Capacitance of the gold electrode in 0.5 M H_2SO_4 solution: a.c. impedance studies. *J. Electroanal. Chem.* **388,** 69–79
65. Wang, Y., and Hu, S. (2006) A novel nitric oxide biosensor based on electropolymerization poly(toluidine blue) film electrode and its application to nitric oxide released in liver homogenate. *Biosens. Bioelectron.* **22,** 10–17
66. Lim, M. D., Lorkovic, I. M., and Ford, P. C. (2005) The preparation of anaerobic nitric oxide solutions for the study of heme model systems in aqueous and nonaqueous media: Some consequences of NOx impurities. in *Nitric Oxide: Part E* (Packer, L., and Cadenas, E., eds) pp. 3–17, Elsevier Academic Press Inc., San Diego
67. Young, C. L. (1981) *IUPAC solubility data series. Oxides of Nitrogen*, Pergamon Press, Oxford